Supporting Information

Studies on the Affinity of 6-[(*n*-(Cyclo)aminoalkyl)oxy]-4*H*-chromen-4-ones for Sigma 1/2 Receptors

Winnie Deuther-Conrad,*[,Ψ] Daniel Diez-Iriepa,[†] Isabel Iriepa,[†] Francisco López-Muñoz,[§], María Angeles Martínez-Grau,[⊥] Michael Gütschow*[,◊] and José Marco-Contelles,*[,‡]

[Ψ] Helmholtz-Zentrum Dresden-Rossendorf, Institute of Radiopharmaceutical Cancer Research, Department of Neuroradiopharmaceuticals, 04318 Leipzig, Germany

[†] Department of Organic and Inorganic Chemistry, University of Alcalá, Ctra. Madrid-Barcelona, Km. 33,6, 28871 Alcalá de Henares, Madrid, Spain

[§] Faculty of Health, Camilo José Cela University of Madrid (UCJC), Spain; Neuropsychopharmacology Unit, "Hospital 12 de Octubre" Research Institute, Madrid, Spain

[⊥] MG Drug Discovery Consulting, C/ Nuria 28 2F, 28034 Madrid, Spain

[◊] Pharmaceutical Institute, Pharmaceutical & Medicinal Chemistry, University of Bonn, An der Immenburg 4, 53121 Bonn, Germany

[‡] Laboratory of Medicinal Chemistry, IQOG, CSIC, C/Juan de la Cierva 3, 28006 Madrid, Spain

Content

1. Effects of chromenones on cholinesterases, monoamine oxidases and σ receptors

Table S1. Inhibition of hAChE, hBuChE, hMAO-B and hMAO-A (IC_{50} ± SE)[a] as well as human σ_1 ($h\sigma_1$) and rat σ_2 ($r\sigma_2$) affinity values (K_i ± SE) of chromenones **1-22**.

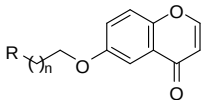

compd		n	hAChE[a]	hBuChE[a]	hMAO-B[a]	hMAO-A[a]	$h\sigma_1$	$r\sigma_2$
1		1	15.7 ± 2.1 µM	30.0 ± 1.7 µM	v.n.d.[b]	n.i.[c]	2,870 nM	12,500 nM
2		2	59.0 ± 6.2 µM	n.i.	v.n.d.	n.i.	499 nM	23,900
3		3	3.74 ± 0.25 µM	n.i.	19.6 ± 0.9 µM	v.n.d.	227 nM	3,110
4		4	7.20 ± 1.19 µM	78.1 ± 14.2 µM	v.n.d.	v.n.d.	87.0 nM	1,450
5		1	17.2 ± 3.9 µM	87.3 ± 12.5 µM	v.n.d.	n.i.	825 ± 146 nM	9,070 nM
6		2	15.9 ± 2.0 µM	n.i.	v.n.d.	n.i.	65.5 ± 4.5 nM	2,890 nM
7		3	5.58 ± 0.49 µM	87.5 ± 11.8 µM	7.20 ± 0.41 µM	v.n.d.	309 ± 45 nM	1,970 ± 1,400 nM
8		4	5.50 ± 0.55 µM	44.8 ± 2.8 µM	v.n.d.	v.n.d.	213 nM	490 nM
9		1	n.i.	n.i.	6.73 ± 0.80 µM	v.n.d.	>10,000 nM	>10,000 nM
10		2	n.i.	n.i.	1.18 ± 0.04 µM	1.70 ± 0.22 µM	245 nM	22,500 nM
11		3	33.5 ± 4.3 µM	n.i.	v.n.d.	v.n.d.	23,9 ± 9,7 nM	14,600 nM
12		4	96.2 ± 7.7 µM	n.i.	v.n.d.	v.n.d.	19.6 ± 3.2 nM	2,630 ± 1,200 nM
13		1	72.9 ± 3.9 µM	n.i.	v.n.d.	n.i.	604 nM	14,200 nM
14		2	65.1 ± 11.4 µM	n.i.	v.n.d.	n.i.	809 nM	17,100 nM
15		4	25.8 ± 2.0 µM	n.i.	v.n.d.	n.i.	82.5 nM	4100 nM

Table S1. Continuation.

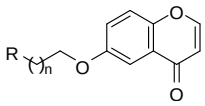

compd		n	hAChE[a]	hBuChE[a]	hMAO-B[a]	hMAO-A[a]	$h\sigma_1$	$r\sigma_2$
16		1	33.6 ± 3.7 µM	n.i.[c]	v.n.d.[b]	n.i.	12,100 nM	30,000 nM
17		2	30.0 ± 3.1 µM	n.i.	v.n.d.	n.i.	1,220 nM	8,360 nM
18		4	6.33 ± 0.77 µM	75.6 ± 13.4 µM	v.n.d.	n.d.	218 nM	2,500 nM
19		1	24.8 ± 2.7 µM	70.0 ± 5.4 µM	3.99 ± 0.42 µM	v.n.d.	113 ± 28 nM	1,620 nM
20		2	10.6 ± 2.2 µM	25.0 ± 4.7 µM	v.n.d.	v.n.d.	27.2 ± 6.8 nM	750 ± 250 nM
21		3	8.62 ± 2.4 µM	48.5 ± 3.9 µM	v.n.d.	v.n.d.	104 nM	1,090 nM
22		4	14.2 ± 2.7 µM	n.i.	v.n.d.	v.n.d.	134 nM	583 nM
haloperidol			n.d.[d]	n.d.	n.d.	n.d.	3.53 ± 0.47 nM	20.5 ± 1.0 nM
SA4503			n.d.	n.d.	n.d.	n.d.	3.77 ± 0.11 nM	n.d.

[a] Data taken from ref 1, which is ref 26 in the main body of the publication.

[b] v.n.d. (values not determined). IC_{50} values have not been determined. Residual activity of MAO-A and MAO-B @ an inhibitor concentration of 10 µM was between 95% and 48%. Data are listed in ref 1.

[c] n.i. (no inhibition) refers to IC_{50} >100 µM (for AChE and BChE) and to >95% residual activity @ 10 µM (for MAO-A).

[d] n.d. (not determined).

2. Determination of hσ$_1$ and rσ$_2$ affinity values of chromenones 1-22

To estimate the binding potential of the test compounds towards σ_1 and σ_2 receptors, radioligand displacement assays were performed using suitable radioligands and target preparations.[2,3] Inhibition constants K_i towards human σ_1 and rat σ_2 receptors are listed in Table 1 and Table S1. To assess the σ_1 affinity, increasing concentrations of the respective test compound (10^{-11} M – 10^{-5} M) were co-incubated with the selective σ_1 receptor ligand (+)-[^{3}H]pentazocine (PerkinElmer LAS GmbH, Rodgau-Juegesheim, Germany; A_M = 995 GBq/mmol) at a single concentration (~ 5 nM) and cell membrane homogenates obtained from HEK293 cells stably transfected with the human σ_1 receptor (provided by Olivier Soriani, Institut de Biologie Valrose, Nice, France) in binding buffer (50 mM TRIS-HCl, pH 7.4, 120 mM NaCl, 5 mM KCl, 2 mM $CaCl_2$, 1 mM $MgCl_2$) at room temperature for 2 hours.

To assess the σ_2 receptor affinity, increasing concentrations of the respective test compound (10^{-11} M – 10^{-5} M) were co-incubated with the non-selective σ_1/σ_2 ligand (+)-[^{3}H]DTG (American Radiolabeled Chemicals, Inc., St. Louis, MO, USA; A_M = 1850 GBq/mmol) at a single concentration (~ 3 nM) in the presence of 10 µM dextrallorphan (obtained from F. Hoffmann-La Roche Ltd, Basel, Switzerland) to mask σ_1 receptor binding sites and rat liver membrane homogenates obtained from female SPRD rats in binding buffer (50 mM TRIS-HCl, pH 7.4) at room temperature for 2 hours.

K_i values determined by three independent experiments are reported as mean ± SD, and K_i values estimated from two independent experiments are reported as mean value. Each experiment was performed in triplicate.

Nonspecific binding of both radioligands was determined by co-incubation with 10 µM haloperidol. The incubations were terminated by filtration via GF/B glass fiber filters (48-Sample Semi-Auto Harvester; Brandel, Gaithersburg, MD, USA) and filter-bound radioactivity was quantified by liquid scintillation counting (Hidex 600 SL; Turku, Finland). The inhibition binding data were expressed as % specific binding of the radioligand vs. a logarithmic molar concentration of the test compound, and the inhibition curve was generated by nonlinear regression using the "one-site competition" equation in GraphPad Prism (Prism 3.0; GraphPad Software, San Diego, CA, USA). From the IC_{50} values, the inhibition constants K_i were calculated using the Cheng-Prusoff equation implemented in GraphPad Prism (KD, (+)-[^{3}H]pentazocine, σ_1 = 33 nM; KD, [^{3}H]DTG, σ_2 = 29 nM).

Experiments to evaluate the S1RA affinity the binding affinity of the target-specific radioligands have been performed in the same experimental setting used to determine the affinity of the test compounds. K_D values were determined by homologous binding experiments ((+)-pentazocine vs. (+)-[^{3}H]pentazocine and DTG vs. [^{3}H]DTG) and estimated according to the converted Cheng-Prusoff equation $K_D = IC_{50}$ – radioligand (M).[4]

Table S2. Overview of the K_D and K_i values of the target-specific radioligands (+)-[^{3}H]pentazocine (σ_1 receptor) and [^{3}H]DTG (σ_2 receptor) and reference compounds haloperidol, **S1RA**, and (±)-PPCC determined herein along with values reported in the literature.

	σ_1 receptor (HZDR: human)	σ_2 receptor (HZDR: rat)
pentazocine	K_D: 34.6 nM K_D: 35 nM[5]	K_i: 5860 nM K_i: 728 nM[6]
DTG	n.d.	K_D: 28.5 nM K_i: 39.9 nM[6] K_i: 58.4 nM[7] K_i: 34.6 nM[8] K_i: 150 nM[2]
haloperidol	K_i: 4.99 nM K_i: 6.44 nM[5] K_i: 1.12 nM[6]	K_i: 20.5 nM K_i: 221 nM[7] K_i: 41.7 nM[8]
S1RA	K_i: 5.07 nM K_i: 17.0 nM[9]	K_i: 3720 nM K_i: > 1000 nM[9]
rac-PPCC	K_i: 11.4 nM K_i: 1.9 nM[10]	K_i: 47.4 nM

3. Cytotoxicty of ligands 7, 12, 20, and standards NE-100, S1RA, and SA4503

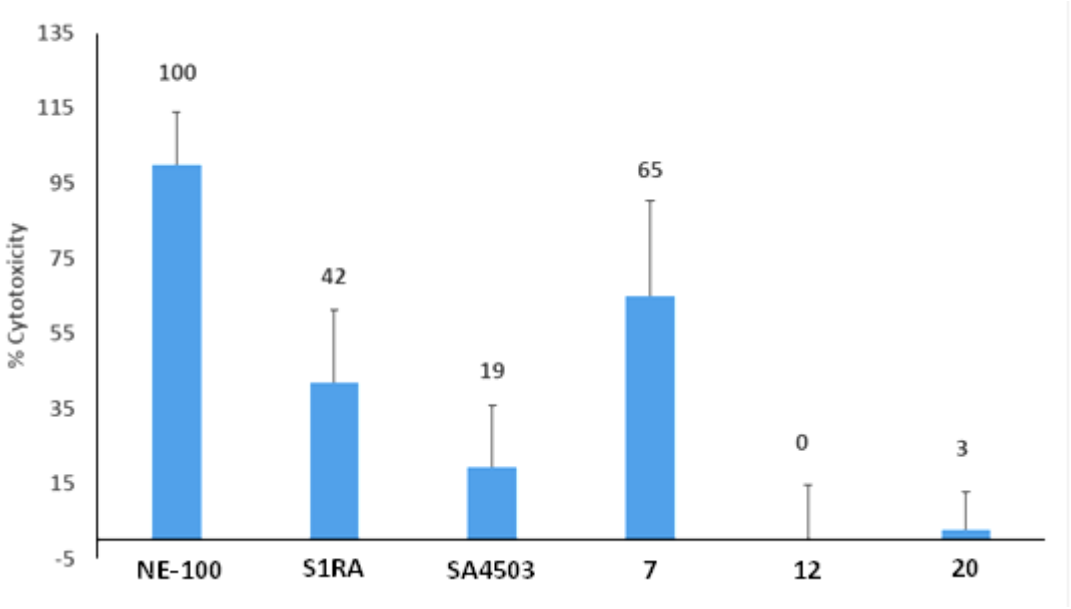

Figure S1. Evaluation of the cytotoxicity of sigma receptor ligands towards SH-SY5Y cells as obtained from the MTT assay. SH-SY5Y cells were treated with test compounds **7**, **12** and **20** and reference compounds (50 µM) for 48 hours. Cell viability was assessed afterwards by an MTT-based cell proliferation assay (CellTiter 96® Non-Radioactive Cell Proliferation Assay; Promega), and cytotoxicity was calculated as % of NE-100 cytotoxicity. **NE-100** and **S1RA** were chosen as references for antagonistic σ_1 receptor ligands antagonist possessing high toxicity. The σ_1 receptor ligands agonist **SA4503** displays low toxicity. Hence, antagonistic effects were concluded for **7**, and agonistic effects for **12** and **20**.

4. Docking of azepane 20 at the σ_1 receptor

To investigate the potential binding mode, the most active compounds **12** and **20** were docked into the σ_1 receptor protein. A validated three-dimensional model of the σ_1 receptor based on the crystal structure of the human σ_1 receptor model bound to the antagonist PD144418 was used.[11] In the model, the receptor flexibility was introduced allowing each ligand to adapt to the catalytic site by the rearrangement of twelve side chains residues in the target. The docking process was executed using AutoDock Vina software.[12] The binding pocket primarily consists of hydrophobic residues Val84, Trp89, Met93, Leu95, Leu105, Leu182, Phe107, Ile124, Trp164, and Tyr103 with the exception of two acidic residues, Glu172 and Asp126.

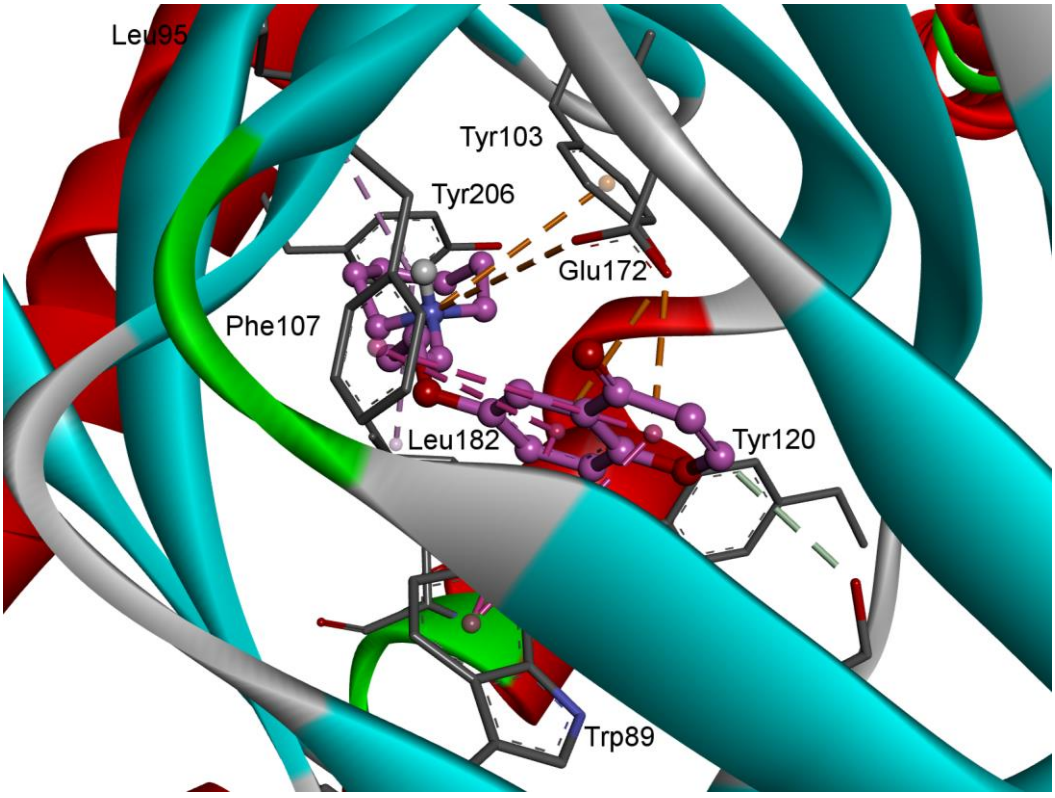

Figure S2. Modeled complex of the σ_1 receptor with compound **20** (pink), showing the key interactions.

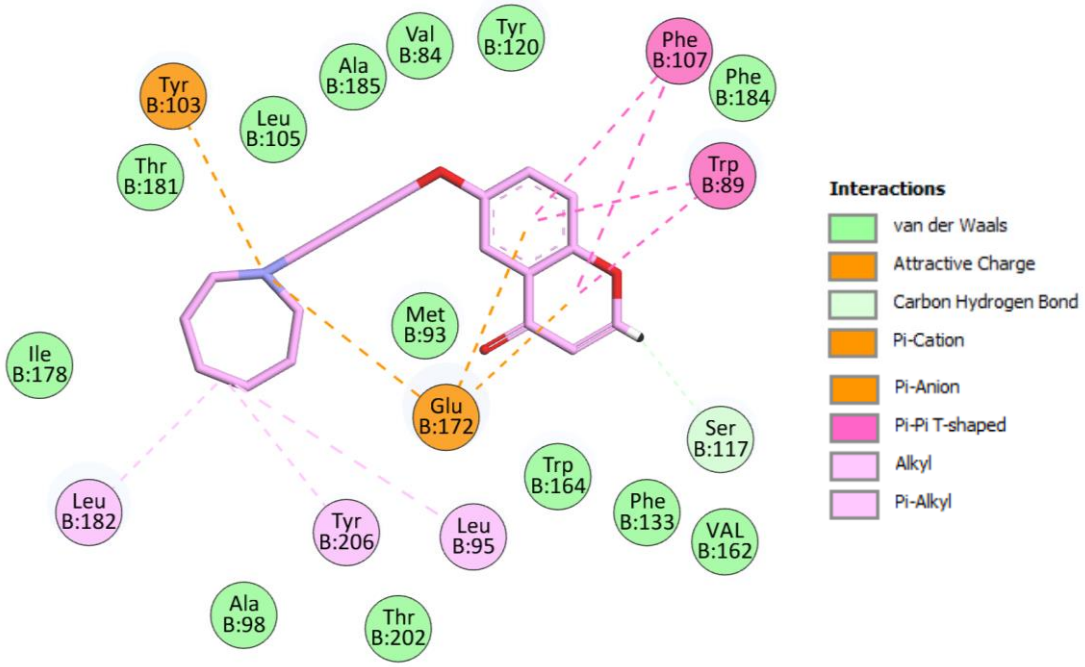

Figure S3. 2D schematic view of the interactions between **20** and the σ_1 receptor.

The detailed inspection of the binding pose of a lower-affinity compound **20** reveals that this molecule adopts a reverse orientation with respect to that assumed for **12.** Accordingly, the chromenone moiety is encased in the hydrophobic cavity lined by residues Val84, Trp89, Phe133, Ser117, Val162, Trp164, Phe184 and Tyr120. Two key interactions between the chromenone moiety and the receptor are established. This moiety is stabilized by π–π T-shaped interactions with Phe107 and Trp89. Any contact with Asp126 is lacking while retaining interactions with Glu172, being the chromenone moiety that establishes a π-anion interactions with this critical amino acid (Figure S2). The protonated nitrogen of azepane moiety undergoes a π-cation interaction with Tyr103 and an attractive charge interaction with the key amino acid, Glu172. The aliphatic portion of this heterocycle is engaged in hydrophobic alkyl interactions with residues Leu95 and Leu182 as well as π-alkyl interaction with Tyr206 (Figure S3). Compound **20** mapped all Glennon's pharmacophore features with a positive ionizable group at the basic azepane nitrogen atom and two opposite hydrophobic regions. The aliphatic portion of azepine ring has at a distance of 3.2 Å to the basic nitrogen and the chromenone moiety a distance of 7.2 Å.

Experimentals. Compounds **12** and **20** as protonated amines were prepared with Discovery Studio, version 2.1, software package, using standard bond lengths and bond angles. The molecular geometries of the compounds were energy-minimized using the adopted-based Newton-Rapson algorithm until the rms gradient was below 0.01 kcal/mol/Å^2. Three-dimensional crystal structure of the hσ_1 receptor bound to the antagonist PD144418 (PDB: 5HK1) was retrieved from the Protein Data Bank (PDB) and chain B of the receptor was extracted from the 5HK1 structure for further modeling. Water molecules, heteroatoms, any co-crystallized solvent and the ligand were removed

prior to use the protein model tool in Discovery Studio, version 2.1, software package to assign proper bonds, bond orders, hybridization and charges. After that, hydrogens and partial charges for proteins and ligands using Gasteiger charges were added using AutoDockTools (ADT; version 1.5.4). Docking approach included protein flexibility through a set of different conformations of selected side chains into the target macromolecule. The ligand was also allowed to change its conformation during the docking process. Using the AutoTors module, we have chosen as flexible twelve amino-acids side chains that could allow the ligand enter or exit the site: Tyr103, Glu172, Phe107, Asp126, Val152, Phe146, Gln135, His154, Glu158, Ser117, Tyr120 and Tyr206. The docking box was displayed using ADT and positioned at the middle of the protein (x = -6.978; y = 20.413; z = -27.539). A grid box of 28 × 22 × 34 with grid point spacing of 1 Å, was used. Docking was performed with the default Autodock Vina[12] settings except num_modes, which was set to 40. The more energetically favorable conformation was selected as the best pose. Discovery Studio software was also used to process the docking results.

5. Virtual ADME of morpholine and azepane derivatives 12 and 20

In order to evaluate the drug likeness and the potential ability to cross the BBB, the compounds **12** and **20** were also *in silico* scored for their physiochemical and pharmacokinetic parameters (ADME) by using the QikProp software [QikProp, version 3.8, Schrodinger, LLC, New York, NY, 2013]. Results are summarized in Table S3.

All calculated descriptors and properties were within the expected thresholds. Some parameters should be discussed as follows. Compounds were found to have no Lipinski rule[13] violations thus proving their drug-likeness properties. They were also predicted to have permeability to the blood-brain barrier. Molecular volume (MW) of a compound is a crucial factor for binding in the active site. It was found that compounds **12** and **20** have the volume 1042.539 and 1018.677 $Å^3$, respectively (the reference value of molecular volume is 500 - 2000 $Å^3$). The lipophilicity of organic molecules is typically quantified in terms of partition coefficients between aqueous and octanol media (log Po/w). Log Po/w values less than five are considered good. Both compounds were within the limits indicated. The gut-blood barrier permeability using Caco-2 cell permeability (QPPCaco) as model was in the appropriate levels, predicting good intestinal absorption. Aqueous solubility is one of the most important factors affecting drug bioavailability. To be absorbed, a drug must be soluble in water first and then have the opportunity to permeate across biological membranes. Both compounds present solubility values within the limits (-6.5 to 0.5). The most used parameter for Blood Brain (BB) barrier penetration is logBB. The predicted logBB values for compounds **12** and **20** (see Table S3) are in the optimum range (-3 < QPlogBB < 1.2). Further, the prediction for human serum albumin binding using QPlogKhsa, shows that the values for all the inhibitors lie within the expected range (-1.5 to 1.5). The number of likely metabolic reactions, which is necessary for determining the level of accessibility of compounds to their target sites after entering into the blood stream, is also in the recommended range (1−8). Molecules with PSA <100 $Å^2$ are more likely to penetrate the BBB and the most active CNS drugs have PSA lower than 70 $Å^2$. The values of PSA for compounds **12** and **20** are 58.010 and 48.413 A^2. The % oral drug absorption predicted for the tested compounds was highly satisfactory with a high percentage (> 89%) of human oral absorption.

Table S3. Predicted ADME and molecular properties for compounds **12** and **20**.

compd	CNS	MW	SASA	volume	donorHB	accptHB	QPlogPo/w	QPlogS
12	1	317.384	590.354	1042.539	0.000	6.950	2.025	-1.406
20	1	301.385	580.086	1018.677	0.000	5.250	2.724	-2.427

compd	QPlogKhsa	QPPCaco	QPlogBB	metab	%HOA	PSA	ROF	ROT
12	-0.512	705.684	0.001	3	89.786	58.010	0	0
20	-0.041	768.084	0.160	2	94.536	48.413	0	0

CNS: Predicted central nervous system activity on a –2 (inactive) to +2 (active) scale. MW: Molecular weight of the molecule (130.0 - 725.0). SASA: Total Solvent Accessible Surface Area, in square angstroms, using a probe with a 1.4 Å radius (limits 300.0 - 1000.0). volume: Total solvent-accessible volume, in cubic angstroms, using a probe with a 1.4 Å radius (limits 500.0 - 2000.0). donorHB: Estimated number of hydrogen bonds that would be accepted by the solute (limits: 0.0 - 6.0). accptHB: Estimated number of hydrogen bonds that would be donated by the solute (limits: 2.0 - 20.0). QPlogPo/w: Predicted octanol/water partition coefficient (limits -2.0 - 6.5). QPlogS: Predicted aqueous solubility. S, in mol/dm^3, is the concentration of the solute's saturated solution that is in equilibrium with crystalline solid (limits -6.5 - 0.5). QPlogKhsa: Prediction of binding to human serum albumin (limits -1.5 - 1.5). QPPCaco: Predicted apparent Caco-2 cell permeability in nm/sec. Caco-2 cells is a model for the gut-blood barrier. QikProp predictions are for non-active transport. (< 25 poor, > 500 great). QPlog BB: Predicted brain/blood partition coefficient (limits -3.0 – 1.2). metab: Number of likely metabolic reactions (limits 1-8). HOA: Predicted qualitative Human Oral Absorption on 0 to 100% scale. PSA: Van der Waals surface area of polar nitrogen and oxygen atoms (limits 7.0 - 200.0). ROF: Number of violations of Lipinski's Rule Of Five. ROT: Number of violations of Jorgensen's Rule of Three.[14,15] (QPlogS > -5.7, QPCaco > 22 nm/s, number of primary metabolites < *7*).

6. References

(1) Lemke, C.; Christmann, J.; Yin, J.; Alonso, J. M.; Serrano, E.; Chioua, M.; Ismaili, L.; Martínez-Grau, M. A.; Beadle, C. D.; Vetman, T.; Dato, F. M.; Bartz, U.; Elsinghorst, P. W.; Pietsch, M.; Müller, C. E.; Iriepa, I.; Wille, T.; Marco-Contelles, J.; Gütschow, M. Chromenones as multineurotargeting inhibitors of human enzymes. *ACS Omega* **2019**, *4*, 22161–22168.

(2) Chu, U. B.; Ruoho, A. E. Sigma receptor binding assays. 2015, *Curr. Protoc. Pharmacol.* **2015**, *71*, 1.34.1–1.34.21.

(3a) Tian, J.; He, Y.; Deuther-Conrad, W.; Fu, H.; Xie, F.; Zhang, Y.; Wang, T.; Zhang, X.; Zhang, J.; Brust, P.; Huang, Y.; Jia, H. Synthesis and evaluation of new 1-oxa-8-azaspiro[4.5]decane derivatives as candidate radioligands for sigma-1 receptors. *Bioorg Med Chem.* **2020**, *28*, 115560. (b) Roslin, S.; De Rosa, M.; Deuther-Conrad, W.; Eriksson, J.; Odell, L. R.; Antoni, G.; Brust, P.; Larhed, M. Synthesis and in vitro evaluation of 5-substituted benzovesamicol analogs containing N-substituted amides as potential positron emission tomography tracers for the vesicular acetylcholine transporter. *Bioorg Med Chem.* **2017**, *25*, 5095–5106.

(4) Motulsky, H. The GraphPad Guide to Analyzing Radioligand Binding Data, GraphPad Software, Inc., San Diego, CA., 1996.

(5) Ramachandran, S.; Lu, H.; Prabhu, U.; Ruoho, A. E. Purification and characterization of the guinea pig sigma-1 receptor functionally expressed in *Escherichia coli*. *Protein Expr. Purif.* **2007** *51*, 283–292.

(6) Lever, J. R.; Gustafson, J. L.; Xu, R.; Allmon, R. L.; Lever, S. Z. Sigma1 and sigma2 receptor binding affinity and selectivity of SA4503 and fluoroethyl SA4503. *Synapse* **2006**, *59*, 350–358.

(7) Vilner, B. J.; Bowen, W. D. Modulation of cellular calcium by sigma-2 receptors: release from intracellular stores in human SK-N-SH neuroblastoma cells. *J. Pharmacol. Exp. Ther.* **2000**, *292*, 900–911.

(8) Colabufo, N. A.; Berardi, F.; Contino, M.; Niso, M.; Abate, C.; Perrone, R.; Tortorella, V. Antiproliferative and cytotoxic effects of some sigma2 agonists and sigma1 antagonists in tumour cell lines. *Naunyn Schmiedebergs Arch. Pharmacol.* **2004**, *370*, 106–113.

(9a) Romero, L.; Zamanillo, D.; Nadal, X.; Sánchez-Arroyos, R.; Rivera-Arconada, I.; Dordal, A.; Montero, A.; Muro, A.; Bura, A.; Segalés, C.; Laloya, M.; Hernández, E.; Portillo-Salido, E.; Escriche, M.; Codony, X.; Encina, G.; Burgueño, J.; Merlos, M.; Baeyens, J. M.; Giraldo, J.; López-García, J. A.; Maldonado, R.; Plata-Salamán, C. R.; Vela J. M. Pharmacological properties of S1RA, a new sigma-1 receptor antagonist that inhibits neuropathic pain and activity-induced spinal sensitization. *Br. J. Pharmacol.* **2012**, *166*, 2289–2306. (b) Díaz, J. L.; Cuberes, R.; Berrocal, J., Contijoch, M.; Christmann, U.; Fernández, A.; Port, A.; Holenz, J.; Buschmann, H.; Laggner, C.; Serafini, M. T.; Burgueño, J.; Zamanillo, D.; Merlos, M.; Vela, J. M.; Almansa, C. Synthesis and biological evaluation of the 1‑arylpyrazole class of σ1 receptor antagonists:

identification of 4‑{2-[5-methyl-1-(naphthalen-2-yl)-1*H*‑pyrazol-3-yloxy]ethyl}morpholine (S1RA, E‑52862). *J. Med. Chem.* **2012**, *55*, 8211−8224.

(10) Prezzavento, O.; Parenti, C.; Marrazzo, A.; Ronsisvalle, S.; Vittorio, F.; Aricò, G.; Scoto, G. M.; Ronsisvalle, G. A new sigma ligand, (+/-)-PPCC, antagonizes kappa opioid receptor-mediated antinociceptive effect. *Life Sci.* **2008**, *82*, 549−553.

(11) Bautista-Aguilera, O. M.; Budni, J.; Mina, F.; Medeiros, E. B.; Deuther-Conrad, W.; Entrena, J. M.; Moraleda, I.; Iriepa, I.; Lopez-Munoz, F.; Marco-Contelles, J. Contilisant, a tetratarget small molecule for Alzheimer's disease therapy combining cholinesterase, monoamine oxidase inhibition, and H3R antagonism with S1R agonism profile. *J. Med. Chem.* **2018**, *61*, 6937–6943.

(12) Trott, O.; Olson, A. J. AutoDock Vina: Improving the speed and accuracy of docking with a new scoring function, efficient optimization, and multithreading. *J. Comput. Chem.* **2010**, *31*, 455–461.

(13) Lipinski, C. A.; Lombardo, F.; Dominy, B. W.; Feeney, P. J. Experimental and computational approaches to estimate solubility and permeability in drug discovery and development settings. *Adv. Drug Delivery Rev*. **2001**, *46*, 3–26.

(14) Duffy, E. M.; Jorgensen,W. L. Prediction of Properties from Simulations: Free Energies of Solvation in Hexadecane, Octanol, and Water, *J. Am. Chem. Soc.* **2000**, *122*, 2878–2888.

(15) Jorgensen, W. L.; Duffy, E. M. Prediction of Drug Solubility from Monte Carlo Simulations. *Bioorg. Med. Chem. Lett*. **2000**, *10*, 1155–1158.